

Energy band dispersion in well ordered N,N'-dimethyl-3,4,9,10-perylenetetracarboxylic diimide films

G. N. Gavrilin,^{a)} H. Mendez, T. U. Kampen, and D. R. T. Zahn
Institute für Physik, Technische Universität Chemnitz, D-09107, Chemnitz, Germany

D. V. Vyalikh
Institut für Festkörperphysik, Technische Universität Dresden, D-01062, Dresden, Germany

W. Braun
BESSY GmbH, Albert-Einstein-Straße 15, D-12489 Berlin, Germany

(Received 22 March 2004; accepted 6 August 2004)

The electronic properties of well ordered N,N'-dimethyl-3,4,9,10-perylenetetracarboxylic diimide (DiMe-PTCDI) films prepared on sulfur passivated GaAs(001) substrates were studied by means of photoemission spectroscopy. From the photon energy dependence of normal emission spectra an intermolecular energy band dispersion of about 0.2 eV was determined for the highest occupied molecular orbital (HOMO). Simulation of the density of states reveals that the HOMO band has a single π -character. The observed energy band dispersion thus originates from the intermolecular π - π interaction and is modeled using the tight binding model. The analysis provides a value of 0.04 eV for the transfer integral. The inner potential was treated as a fitting parameter such that the expected periodicity of the dispersion in the reciprocal space was obtained. © 2004 American Institute of Physics. [DOI: 10.1063/1.1800273]

Organic semiconductors have become a very active area of research in the last decade, mainly due to their potential applications in (opto-)electronic devices. A major branch of functional organic materials with interesting properties are the π -conjugated system.¹ Well ordered organic crystals or thin films are beneficial for achieving high carrier mobilities.²⁻⁴ The ability of these materials to transport charges (holes and electrons) due to the π -orbital overlap of neighboring molecules provides their semiconducting and conducting properties. The self-assembling or ordering of these organic materials enhances this π -orbital overlap and is the key to improvement in carrier mobilities.

Many organic crystals are formed by regularly repeating a small unit along one direction. In such systems the electronic energy levels of the units with the same energy may interact via the outermost orbitals leading to a splitting of the respective energy levels. The width of the resulting energy band then depends on the magnitude of interaction.

We can experimentally probe the energy dispersion using angular resolved ultraviolet photoemission spectroscopy⁵⁻⁷ or by measuring the energy dependence of the valence electrons emitted normal to the substrate surface^{8,9} in order to determine the dispersion parallel and perpendicular to the sample surface, respectively. For organic semiconductors the intermolecular energy band dispersion is difficult to observe since the width of the bands is expected to be very small due to the weak van der Waals (vdW) interaction.

Experiments for π -conjugated polymers⁸⁻¹⁰ and also for small molecule films like C₆₀¹¹ revealed bandwidths of about 0.4 eV. Recently the intermolecular energy dispersion was measured for the archetypal organic semiconductor 3,4,9,10-

perylenetetracarboxylic dianhydride (PTCDA) deposited onto MoS₂ to be 0.2 eV.¹²

Here the photon energy dependence of normal emission spectra of N,N'-dimethyl-3,4,9,10-perylenetetracarboxylic diimide (DiMe-PTCDI) thin films is determined. The overall energy shift of the highest occupied molecular orbital (HOMO) feature which originates from the HOMO-HOMO interaction in the well ordered DiMe-PTCDI films is found to be about 0.2 eV. This reveals a small energy band dispersion for wave vectors varied along the direction perpendicular to the sample surface. Moreover, the spectral features in the photoemission spectra are assigned by comparing them with a simulated density of states (DOS).

The perpendicular component of the initial state wave vector is usually determined assuming free electron-like final states and an inner potential V_0 which has to be determined. V_0 is treated as a fit parameter to obtain the expected periodicity of the dispersion in reciprocal space. As previously reported,¹² the tight binding model is a suitable approach to determine such energy-band dispersion. The same approach is applied here taking into account the complementary results providing information on the intermolecular spacing.

Thin DiMe-PTCDI films were prepared by organic molecular beam deposition onto sulphur passivated, tellurium doped *n*-GaAs(100) substrates (Freiberger Compound Materials GmbH, $N_D = 2 \times 10^{17} \text{ cm}^{-3}$) kept at room temperature. Additional details about the passivation process and surface reconstruction are given elsewhere.¹³ The DiMe-PTCDI material was purchased from Sensient GmbH, further being purified twice by sublimation at 575 K under high vacuum ($\sim 10^{-4}$ Pa).

The photoemission spectra of DiMe-PTCDI films with a total thickness of 15 nm were measured using a CLAM 4 analyzer at the Russian-German beamline at BESSY. Monochromatized synchrotron radiation in the range of $h\nu = 35-90$ eV obtained using a plane grating monochromator

^{a)} Author to whom correspondence should be addressed; electronic mail: gianina-nicoleta.gavrilin@physik.tu-chemnitz.de

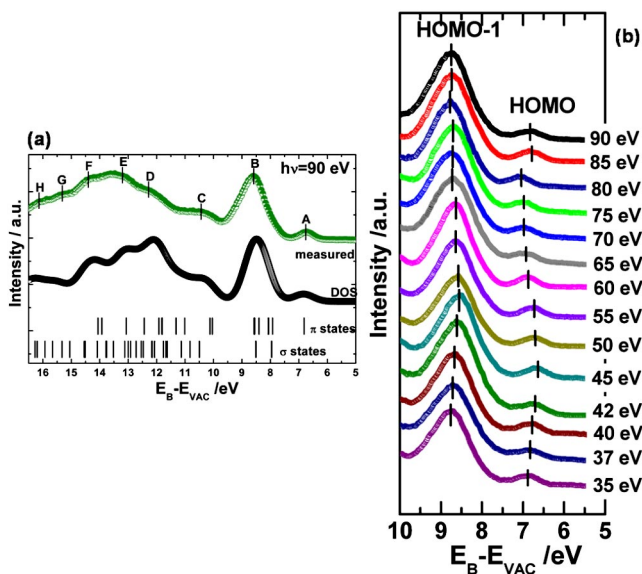


FIG. 1. (a) Valence band and DOS of DiMe-PTCDI thin films and calculated DOS. The MO energies are shown by vertical bars. The DOS curve was calculated by Gaussian broadening of the energy levels with a FWHM of 0.6 eV. The HOMO is a π -derived state while HOMO-1 is dominated by σ -dominant states. (b) Measured valence band spectra of a DiMe-PTCDI thick film in the photon energy range of $35 \leq h\nu \leq 90$ eV.

served as a light source. The spectra were measured at normal emission with an incident angle of light of 65° with a total resolution over the whole energy range used in the present measurements, better than 0.1 eV as estimated from the Fermi edge of silver.

HOMO features were fitted using Gaussian functions in order to obtain their energy positions in the spectra accurately.

Molecular orbital calculations were performed using the Gaussian '98 package¹⁴ with the B3LYP method and 6-311G(d) basis set to describe the core orbitals and the inner and outer part of the valence orbitals. The Levenberg–Marquardt method was used to fit the observed HOMO positions to a cosine function in the tight binding model.

The upper spectrum in Fig. 1(a) shows the measured spectrum of the DiMe-PTCDI film at a photon energy $h\nu = 90$ eV energy. Eight features (A-H) are observable at binding energies with respect to the vacuum level of 6.7, 8.6, 10.4, 12.3, 13.2, 14.4, 15.3, and 16.1 eV, respectively. The HOMO (A) and the HOMO-1 (B) appear as separate peaks while the remaining ones overlap. The vertical bars in Fig. 1(a) represent the calculated binding energies of each molecular orbital (MO) state for a single molecule, while the lower curve shows the calculated density of states (DOS). The DOS was obtained by Gaussian broadening of each orbital energy with a full width at half maximum (FWHM) of 0.6 eV. The value of the Gaussian FWHM was taken equal to the FWHM of the experimentally observed HOMO state. In order to compare the simulated DOS and the measured valence band spectrum the energy scale of the calculated spectrum was shifted by 0.73 eV towards higher binding energies. The value of the Gaussian width represents the spectral broadening due to solid-state effects such as charge-induced intermolecular polarization,¹⁵ vibrational excitations or final-state lifetime¹⁶ and structural disorder if present.

The HOMO originates from a single molecular orbital with π character which is distributed predominantly over the

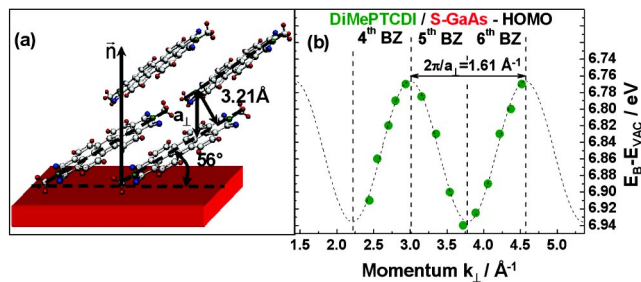


FIG. 2. (a) DiMePTCDI crystal plane and the relative orientation of molecules with respect to the S-GaAs(001) substrates. (b) The experimental dispersion for the HOMO band (filled circles) and the best fit curve (broken line) in the tight binding model.

perylene core. The strong peak at a binding energy of 8.6 eV is characteristic for DiMe-PTCDI and stems from both π and σ bonds in the imide, carboxylic and methyl groups. Above 13.5 eV mostly molecular orbitals with σ character contribute to the spectra.

Figure 1(b) shows the measured valence band spectra in the HOMO and HOMO-1 region and their dependence on energy. The HOMO feature reveals a weak, but clearly observable shift of about 0.2 eV, to the intermolecular π - π interaction. While the dispersion of the HOMO position is obvious, it is much less pronounced for the HOMO-1 feature. This is explained by the higher binding energy and the predominant σ character of the molecular orbitals contributing to HOMO-1.

The measured energy shift was converted into a dispersion relation assuming the three-step model¹⁷ for the photoemission process as well as energy and momentum conservation before and after photoexcitation so that the following relations hold:

$$E_f = h\nu + E_i, k_f^\perp = k_i^\perp + G^\perp, \quad E_{\text{kin}} = E_f, \quad (1)$$

where E_i , E_f , k_i^\perp and k_f^\perp are the electron energies and the wave vectors before and after photoexcitation in the solid, and G^\perp is a reciprocal lattice vector. E_i and E_f are defined relative to the vacuum level such that E_f corresponds to the kinetic energy of the emitted electrons E_{Kin} . Determination of the final momentum k^\perp requires the knowledge of the final state band dispersion $E_f(k_f^\perp)$ which is, however, generally unknown. Therefore, it is commonly assumed that the final state can be approximated by a free electron-like dispersion applying an appropriate inner potential V_0

$$E_f = \hbar^2 k^2 / 2m^* + V_0, \quad (2)$$

where m^* is the effective mass of the electron and V_0 is the constant inner potential in the solid for the final state free-electron-like parabola. Then the following relations are used:

$$E_i = E_{\text{Kin}} - h\nu, \quad (3)$$

$$k_i^\perp = k_f^\perp = [2m^* \times (E_f - V_0)]^{1/2} / \hbar \\ = [2m^* \times (E_{\text{Kin}} - V_0)]^{1/2} / \hbar, \quad (4)$$

where k_i^\perp , k_f^\perp are the normal components of the wave vector before and after the photoexcitation in the solid, respectively. These equations indicate that the values of E_i , and k_i^\perp can be determined from the measured E_{Kin} and $h\nu$. The effective mass of the excited electron m^* is approximated by the mass of free electron m_0 .

The energy band dispersion relation for DiMe-PTCDDI is obtained by applying the one-dimensional (1D) tight binding theory to the HOMO of the perylene core. For the formation of a 1D energy band it is assumed that a unit, i.e., a molecule, is repeating along an axis x with a period a . The interaction only takes place with the nearest neighbors, its strength being defined by the value t , the transfer integral. By analogy to the Hückel theory,¹⁸ the energy E_B for the HOMO is expressed in terms of wave vector k_{\perp} as⁸

$$k_{\perp} = [2m^* \times (h\nu - E_B - V_0)], \quad (5)$$

$$E_B(k_{\perp}) = E_B^0 + 2t \cos(a_{\perp} \times k_{\perp}). \quad (6)$$

Using the normal emission spectra and Eqs. (5) and (6) the energy of the highest valence band and its momentum can be calculated. However, for the experimental determination of the energy band dispersion we need to determine the values of t , a_{\perp} , and V_0 .

Results of Raman, near edge x-ray absorption fine structure (NEXAFS) and infrared spectroscopy¹⁹ revealed that the DiMe-PTCDDI molecules deposited onto S-GaAs(001) are tilted with respect to the substrate surface by an angle of ($56^{\circ} \pm 4^{\circ}$) and are predominantly oriented with their long axis parallel to the [011] direction. With the distance between the intermolecular planes of 3.21 Å, as experimentally determined,²⁰ we can calculate the length of repeating unit (lattice spacing normal to the surface) as $a_{\perp} = 3.9$ Å as depicted in Fig. 2(a).

The results of the best fit for the dispersion along with the experimental data are shown in Fig. 2(b). A cosine fit of the experimental data was performed where the inner potential V_0 and the transfer integral t are the two parameters. The best fit is provided by the following parameters: inner potential $V_0 = 5.3$ eV and transfer integral $t = 0.04$ eV. The HOMO band dispersion in the Fig. 2(b) allows the effective mass of HOMO hole to be determined as $m_h^* = 6.20 m_0$. This value is close to the one derived for PTCDA ($5.28 m_0$) as can be expected due to the similarity of the two perylene derivative.¹² In principle the effective mass value can be employed to calculate the hole mobility in the organic semiconductor. However, this additionally requires the knowledge of the scattering time which is not well known. Therefore we refrain from providing a coarse estimation of the carrier mobility as in the PTCDA case.¹²

As shown in the Fig. 2(b) we succeeded to observe the HOMO band dispersion for DiMe-PTCDDI along surface normal. The energy-band dispersion is extended over three Brillouin zones (4th, 5th, and 6th zone) with a bandwidth of about 0.2 eV.

These results clearly demonstrate the existence of energy-band dispersion similar to that for PTCDA.¹² Here the calculated lattice spacing normal to the surface gives rise to the best fit of the energy dispersion to the experimental data using an inner potential V_0 of -5.1 eV and a transfer integral of 0.04 eV. The inner potential for PTCDA was found to be -5.1 eV from the low energy transmission spectrum for an estimated lattice spacing of 3.8 Å.

The HOMO for both perylene derivatives, DiMe-PTCDDI and PTCDA,²¹ originates from a single molecular orbital with π character which is distributed predominantly over the perylene core. The results for the transfer integral and the inner potential of PTCDA are quite close to the ones of

DiMe-PTCDDI. This supports the reliability of the results since the interacting parts are the perylene cores of the molecules in both cases. The minor differences may be due to the difference of the intermolecular vdW interaction between the stacks of the two molecular films, considering that the lattice spacing is larger for DiMe-PTCDDI than the one determined for PTCDA.

In this work we present valence band spectra from well ordered films of N,N'-dimethyl-3, 4,9, 10-perylenetetracarboxylic diimide. From the photon energy dependence of the highest occupied molecular orbital (HOMO), an energy dispersion of 0.2 eV was experimentally observed and attributed to the HOMO-HOMO interaction. The observed energy shift of the HOMO is explained in terms of k conservation rule in the photoexcitation process with a transfer integral t of 0.04 eV and inner potential V_0 equal to -5.3 eV. The lattice spacing normal to the surface was calculated taking into account the molecular orientations determined from NEXAFS, Raman and infrared spectroscopy.

This work was supported by the BMBF (No. 05 KSIOCA/1) and the EU funded Human Potential Research Training Network DIODE [Contract No. HPRN-CT-1999-00164] for financial support. The authors also thank Hiroyuki Yamane for the fruitful discussions.

¹M. Pope and C. E. Swenberg, *Electronic Processes of organic crystals and polymers*, 2nd ed. (Oxford University Press, New York, 1999).

²C. Dimitrakopoulos, A. Brown, and A. Pomp, *J. Appl. Phys.* **80**, 2501 (1996).

³J. Meyer zu Herindorf, M. C. Reuter, and R. M. Tromp, *Nature (London)* **412**, 517 (2001).

⁴G. Horowitz, R. Hajillaoui, D. Fichou, and El Kassmi, *J. Appl. Phys.* **85**, 3202 (1999).

⁵T. Permien, R. Engelhardt, C. A. Feldmann, and E. E. Koch, *Chem. Phys. Lett.* **98**, 527 (1983).

⁶S. Hasegawa, T. Mori, K. Imaeda, S. Tanaka, Y. Yamashita, H. Inokuchi, H. Fujimoto, K. Seki, and N. Ueno, *J. Chem. Phys.* **100**, 6968 (1994).

⁷K. K. Okudaira, S. Hasegawa, H. Ishii, K. Seki, Y. Harada, and N. Ueno, *J. Appl. Phys.* **85**, 6453 (1999).

⁸S. Narioka, H. Ishii, K. Edamatsu, K. Kamiya, S. Hasegawa, N. Ueno, and K. Seki, *Phys. Rev. B* **52**, 2362 (1995).

⁹T. Miyamae, S. Hasegawa, D. Yoshimura, H. Ishii, N. Ueno, and K. Seki, *J. Chem. Phys.* **112**, 333 (2000).

¹⁰N. Ueno, K. Seki, N. Sato, H. Fujimoto, T. Kuramochi, K. Sugita, and H. Inokuchi, *Phys. Rev. B* **41**, 1176 (1990).

¹¹G. Gensterblum, J. J. Pireaux, P. A. Thyry, R. Caudano, T. Buslaps, R. L. Johnson, G. Le Lay, V. Aristov, R. Günther, A. Taleb Ibrahim, G. Indlekofer, and Y. Petroff, *Phys. Rev. B* **48**, 14756 (1993).

¹²H. Yamane, S. Kera, K. K. Okudaira, D. Yoshimura, K. Seki, and N. Ueno, *Phys. Rev. B* **68**, 033102 (2003).

¹³D. R. T. Zahn, T. U. Kampen, S. Hohenecker, and W. Braun, *Vacuum* **57**, 139 (2000).

¹⁴Gaussian 98 (Revision A.1), Gaussian, Pittsburgh, PA, 1998.

¹⁵E. V. Tsiper and Z. G. Soos, *Phys. Rev. B* **64**, 195124 (2001).

¹⁶S. Kera, H. Yamane, I. Sakuragi, K. K. Okudaira, and N. Ueno, *Chem. Phys. Lett.* **364**, 93 (2002).

¹⁷K. Seki, N. Ueno, U. O. Karlson, R. Engelhardt, and E. E. Koch, *Chem. Phys.* **105**, 247 (1986).

¹⁸J. J. Pireaux, J. Riga, R. Caudano, J. J. Verbist, J. M. Andre, J. Delhalle, and S. Delhalle, *J. Electron Spectrosc. Relat. Phenom.* **5**, 531 (1974).

¹⁹M. Friedrich, G. Gavrila, C. Himeinschi, T. U. Kampen, A. Y. Kobitski, H. Méndez, G. Salvan, I. Cerrilló, J. Méndez, N. Nicoara, A. M. Baró, and D. R. T. Zahn, *J. Phys.: Condens. Matter* **15**, S2699 (2003).

²⁰E. Hädicke and F. Graser, *Acta Crystallogr., Sect. C: Cryst. Struct. Commun.* **42**, 189 (1986).

²¹S. Kera, H. Setoyama, M. Onoue, K. K. Okudaira, Y. Harada, and N. Ueno, *Phys. Rev. B* **63**, 115204 (2001).